www.czasopisma.pan.pl PAN POLSKA AKADEMIA NAUK www.journals.pan.pl

Arch. Metall. Mater. **63** (2018), 4, 2009-2015

DOI: 10.24425/amm.2018.125137

J. TRZASKA*#

A NEW NEURAL NETWORKS MODEL FOR CALCULATING THE CONTINUOUS COOLING TRANSFORMATION DIAGRAMS

The article shows a new model of Continuous Cooling Transformation (CCT) diagrams of structural steels and engineering steels. The modelling used artificial neural networks and a set of experimental data prepared based on 550 CCT diagrams published in the literature. The model of CCT diagrams forms 17 artificial neural networks which solve classification and regression tasks. Neural model is implemented in a computer software that enables calculation of a CCT diagram based on chemical composition of steel and its austenitizing temperature.

Keywords: CCT diagram, modelling, neural network, heat treatment, steel

1. Introduction

Knowledge of austenite transformation kinetics occurring during continuous cooling of steel from the austenitizing temperature presented at CCT diagrams helps determine the conditions of operations such as hardening, normalising or full annealing. The position and shape of austenite transformation curves marked on CCT diagrams depend primarily on the chemical composition of steel, the starting condition of material and the conditions of austenitizing [1]. Knowledge of transformation of a supercooled austenite occurring in the steel with a known chemical composition is also important during modelling of the heat treatment. Based on CCT diagrams, often parameters of phase transformation models are calculated. The ability to calculate a CCT diagram is an alternative to dilatometric and metallographic investigations. It shortens the time required to get results and reduced the costs of laboratory tests.

In 1944, Payson and Savage published an equation that enabled calculation of the martensitic start transformation temperature M_s based on chemical composition of the steel [2]. The researchers used the multiple regression method and Greninger test results [3], as well as Greninger and Troiano testing [4]. Further regression models were formed based on larger datasets and differed ranges of values of independent variables for which they could be used. In addition to multiple regression, artificial neural networks (ANN) started to be used [5-7].

CCT diagrams are developed in laboratories of many countries and published in atlases, guidebooks and academic works. The collection of data on transformations of a supercooled austenite increases regularly starting from the works of Davenport and Baine [8]. It offers an opportunity to prepare a representative set of data and use regression methods such as artificial neural networks or multiple regression to develop CCT diagram models. New models are still being proposed, based on both theoretical considerations and methods using empirical data. These models can be used in a wide range of mass concentrations of the elements or dedicated to a specific group of steels.

The first original method for calculation of CCT diagrams while using artificial neural networks is shown, among others, in the works of [9-11]. Acquiring new empirical data and analyzing verification calculations made in the next few years convinced the author to reconsider the solutions of that time. The CCT diagram set was largely increased while changing their digitalization, improving the design of artificial neural networks and developing a new base of rules used to determine the temperature of the transformations. As a result, a new neural model of CCT diagrams was developed, which consists of 17 neural networks that solve classification and regression tasks. The model was implemented in a computer software to calculate CCT diagrams.

2. Data and method

It was assumed that a CCT diagram of steel with a known chemical composition, austenitized in set conditions, can be calculated based on results of the models below:

- Start temperature of pearlite transformation into austenite while heating Ac_1,
- Finish temperature of ferrite transformation into austenite while heating Ac_3,

* SILESIAN UNIVERSITY OF TECHNOLOGY, INSTITUTE OF ENGINEERING MATERIALS AND BIOMATERIALS, FACULTY OF MECHANICAL ENGINEERING, 18A KONARSKIEGO STR., 44-100 GLIWICE, POLAND

Corresponding author: jacek.trzaska@polsl.pl

- Maximum temperature at which the austenite is transformed into bainite $B_{s\max}$,
- Martensite start temperature M_s,

and for a determined cooling rate:

- Start and finish temperatures of transformation of: austenite into ferrite F_s, F_f, austenite into pearlite P_s, P_f, austenite into bainite B_s, B_f,
- Start temperature of austenite transformed into martensite $M_s(v_c)$,
- Steel hardness,
- Volume fraction of: ferrite F(%), pearlite P(%), bainite B(%) and martensite M(%).

Calculation of transformation temperature curves on a CCT diagram required transformation temperature to be calculated and the range of cooling rate to be determined. The solution was offered that introduced classifiers to the model. The goal of the classifiers was to determine if the analyzed transformation occurs in a steel with a known chemical composition and known austenitizing temperature under cooling at a set rate. Four classifiers were developed where the dichotomic output variable described the transformation: ferritic (W_f), pearlitic (W_p), bainitic (W_b) and martensitic (W_m). Thus, the data on the type of microstructure constituents occurring in the steel after cooling at a set rate was acquired. The calculations of neural classifiers were used to calculate: the transformations temperature, hardness and volume fraction of structural constituents. According to the assumptions, a neural model of CCT diagrams consisted of 17 neural networks, including four classifiers.

Developing a neural model of CCT diagrams required representative set of empirical data. Preparation of a dataset started from determining the variables representing the model. The selection of independent variables should be supported by knowledge on the modelled process. Also, vectors including examples to calculate model parameters and model testing must include all variables. To satisfy these assumptions, it was necessary to assume simplifications related to the number of variables. The data regarding the austenitization time and austenite grain size was dismissed since it was not provided on most CCT diagrams that were the sources of data. It was assumed that the model independent variables will be the mass concentrations of the elements: C, Mn, Si, Cr, Ni, Mo, V, Cu and austenitizing temperature. Another variable that needed to be included already at digitalization of CCT diagrams was the cooling rate.

The dataset prepared within the work [9] was complemented with new examples. A total of 550 CCT diagrams published in the literature was collected. The range of independent variables for which the developed models can be used was analyzed. It was tested if the examples for developing and testing of a model evenly cover the whole field of approximated functions. Any missing values were complemented or additional conditions restricting the model use were determined. Distributions of independent variables were reviewed based on descriptive statistics, scatter plots and histograms made for one and two variables. Within descriptive statistics the minimum and maximum values, the mean value, standard deviation, median, skewness and kurtosis were analyzed. A verification set consisting of 25 CCT diagrams was created. The data from this set were not used to calculate model parameters. It was only used for numerical verification of developed models.

The range of mass concentrations of the elements and austenitizing temperature in which the model can be used is shown in Table 1. Based on statistical analysis of data, additional conditions restricting the model use were determined (Table 2).

TABLE 1

Ranges of mass concentrations of elements

	Mass fractions of elements, %								T_A,°C
	C	Mn	Si	Cr	Ni	Mo	V	Cu	
min	0.1	0.28	0.13	0	0	0	0	0	780
max	0.68	1.98	1.9	2.5	3.85	1.05	0.38	0.38	1050
T_A – austenitizing temperature, °C									

TABLE 2

Additional conditions for limiting the scope of model application

	Mass fractions of elements, %			
	Mn+Cr	Mn+Cr+Ni	Cr+Ni	Mn+Ni
max	3.6	5.6	5.3	4.5

A dataset prepared to develop the model was divided into the training, validation and testing sets. The data from the training set was used to determine the value of connection weights between neurons while training. The validation set was used to verification the neural network while training, and the testing set was used to verification the quality of a neural network after its design. The ratio of division into sets: training, validation and testing set, was assumed as 2:1:1.

After analyzing the results of initial calculations, further discussion was limited to Multi-Layer Perceptron (MLP) network with one hidden layer.

The design of an artificial neural network, preceded with preparation of dataset was divided into the following stages performed multiple times:

- selection of dependent and independent model variables;
- determining the method for coding nominal variables (if applies);
- determining the number of neurons in the hidden layer;
- determining: the form of error function, activation function, PSP – Post Synaptic Potential function, variable scaling methods;
- training a neural network combined with analyzing the significance of independent variables;
- model evaluation.

The following algorithms to training the artificial neural networks were used: backpropagation (BP), quick propagation (QP), conjugate gradients (CG), Lavenberg-Marquardt (LM), quasi-Newton (QN) and delta-bar-delta (DD). While training, the value of the Root Mean Square (RMS) error was analyzed. A change of the RMS error was noted in the next training epochs

for the training and validation sets. Training was stopped when the error for the validation set increased.

The significance of independent variables was assessed based on the quotient of the estimated error made by a neural network without analyzed variable and an error made by the neural network for all input variables. An independent variable was considered significant if the quotient calculated for the training set and the validation set was higher than 1. The models included only significant variables. The values of statistics used to assess the significance of independent variables on the example of the M_s temperature model is shown in Table 3. The table contains the statistics for variables considered as significant. The error describes an estimated RMS error for a neural network as if the analyzed variable was dismissed.

TABLE 3

Example of significance assessment of independent variables for the Ms temperature model

Data sets	Statistic	Independent variable					
		C	Mn	Cr	Ni	Mo	V
training	error, °C	55.3	23.9	21.5	27.2	19.3	19.6
	ratio	2.91	1.26	1.13	1.43	1.03	1.04
validating	error, °C	57.2	25.1	19.9	23.8	19.7	18.9
	ratio	3.04	1.33	1.05	1.26	1.05	1.03

The start and finish temperature lines of austenite transformation are calculated independently by seven neural networks. It should be assumed that every result is subject to an error which may lead to unsatisfied condition (1):

$$F_s > F_f \geq P_s > P_f \geq B_s \geq B_f \geq M_s \tag{1}$$

On CCT diagrams, transformations of a supercooled austenite occur one by one or are divided by an austenite area. For the same cooling rate, the start and finish of the next transformation may be characterized by the same temperature: $F_f - P_s$, $F_f - B_s$, $P_f - B_s$, $B_f - M_s$. Considering the previous calculation error and condition (1), rules to determine the transformation temperatures shown in a CCT diagram were defined. The algorithm is shown in Figure 1. The rules are performed according to the sequence of numbers 1-4. It was assumed that the same value will be assumed for the transformation finish and start temperature if the absolute difference between the calculated temperatures will be lower than the total of mean absolute errors for respective models. The final temperature was calculated as a weighted average assuming an absolute error E_i as weight (where: $i = F_s, F_f, P_s, P_f, B_s, B_f, M_s$) for individual models.

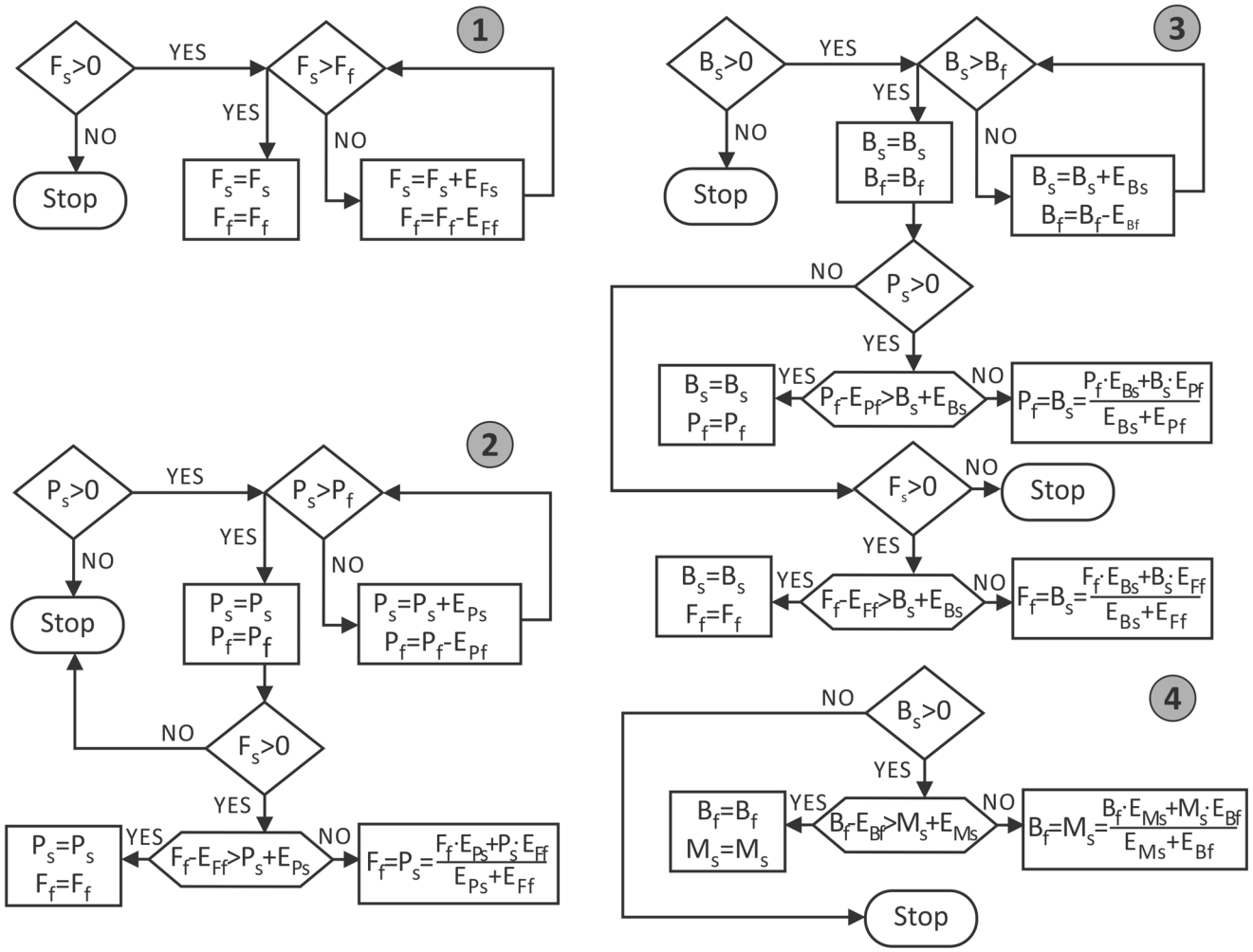

Fig. 1. Algorithm for determining the temperatures of start and finish of the transformations

3. Calculation results

The neural networks in regression tasks were evaluated based on the mean absolute error of neural network forecast, standard deviation of neural network forecast error, Paerson correlation coefficient and the quotient calculated for the standard deviation of the forecast error and the standard deviation of the dependent variable. The quotient of standard deviations allows to relate an error made by the neural network to the range of dependent variable. The ideal value of this statistics is 0. Neural networks in classification tasks were assessed based on the correct classification coefficient and the area under the ROC (Receiver Operating Characteristic) curve. The correct classification coefficient was calculated as the quotient of a number of correct network classifications and all cases in a set. The ROC curve allows to assess the two-state classifier for all possible thresholds determining the border between the classes. In case of an perfect classifier, its value is 1. All statistics were calculated for the training set, validation set and testing set. The network's ability to generalize the knowledge acquired in the training process, is confirmed by similar statistics for the training set, validation set and the testing set, respectively. The better values of statistics for the training set may be a sign of an overfitting neural network. Most important information on neural classifiers and networks performing regression tasks are shown in Table 4 and Table 5. Tables 6-9 show the statistics for evaluating neural networks. The tables provide statistics for the testing set. The hardness model is shown also in the work [12].

TABLE 4

Specifications of the developed classifiers based on neural networks

Dependent variable ANN output	Independent variables ANN inputs	ANN structure	Training method/No of epochs
W_f	C, Mn, Si, Cr, Ni, Mo, V, Cu, T_A, v_c	10-8-1	BP/50, CG/330
W_p		10-8-1	BP/50, CG/119
W_b		10-10-1	BP/50, CG/188
W_m		10-6-1	CG/100
v_c – cooling rate, °/min			

TABLE 5

Specifications of the neural networks used for regression tasks

Dependent variables ANN output	Independent variables ANN inputs	ANN structure	Training method/No of epochs
Ac_1	C, Mn, Si, Cr, Ni, Mo, V, Cu	8-4-1	BP/50, CG/78
Ac_3		8-5-1	BP/50, CG/162
$B_{s\,max}$	C, Mn, Si, Cr, Ni, Mo, V	7-10-1	CG/125 LM/20
M_s	C, Mn, Cr, Ni, Mo, V	6-6-1	LM/296
F_s	C, Mn, Si, Cr, Ni, Mo, V, Cu, T_A, v_c	10-10-1	BP/50, CG/396
F_f		10-9-1	BP/50, CG/307
P_s	C, Mn, Si, Cr, Ni, Mo, V, v_c	8-8-1	LM/760
P_f	C, Mn,Si,Cr,Ni, Mo,V, Cu,T_A,v_c	10-5-1	BP/50, CG/437
B_s	C, Mn, Si, Cr, Ni, Mo, V, T_A, v_c	9-14-1	BP/50, CG/471
B_f	C, Mn, Si, Cr, Ni, Mo, T_A, v_c	8-15-1	QN/534
$M_s(v_c)$	C, Mn, Cr, Ni, Mo, V, Cu, T_A, v_c	9-5-1	LM/460
Hardness	C, Mn, Si, Cr, Ni, Mo, V, Cu, T_A, v_c, W_f, W_p, W_b, W_m	14-10-1	BP/50, CG/489
F(%), P(%), B(%), M(%)		14-16-4	CG/320

TABLE 6

Quality assessment coefficients for models, used as classifiers for determining the types of occurring transformations (testing set)

	Transformation areas, output variable			
	Ferritic W_f	Pearlitic W_p	Bainitic W_b	Martensitic W_m
CCC, %	0.89	0.91	0.84	0.86
ROC	0.957	0.967	0.915	0.934
CCC – Coefficient of correct classifications				

TABLE 7

Statistic values used to evaluate the transformation temperature models (testing set)

Dependent variable	Mean absolute error,°C	Standard deviation of the error,°C	Ratio of standard deviations	Correlation coefficient
Ac_1	12.8	15.9	0.62	0.79
Ac_3	12.5	15.4	0.46	0.90
$B_{s\,max}$	18.6	22.9	0.40	0.92
M_s	13.6	19.1	0.37	0.93
F_s	17.1	23.2	0.44	0.90
F_f	20.1	26.3	0.50	0.86
P_s	14.8	19.0	0.44	0.90
P_f	21.8	28.9	0.56	0.82
B_s	24.2	31.2	0.55	0.83
B_f	25.9	34.3	0.59	0.80
$M_s(v_c)$	15.6	21.4	0.37	0.93

TABLE 8

Statistic values used to evaluate the hardness model (testing set)

	Mean absolute error, HV	Standard deviation of the error, HV	Ratio of standard deviations	Correlation coefficient
Hardness	33.1	48.9	0.30	0.95

TABLE 9

Statistic values used to evaluate model of the microstructural constituents (testing set)

Structural constituent	Mean absolute error,%	Standard deviation of the error,%	Ratio of standard deviations	Correlation coefficient
Ferrite	7.8	12.3	0.48	0.88
Pearlite	6.6	10.9	0.38	0.92
Bainite	12.7	18.0	0.55	0.84
Martensite	8.8	14.2	0.34	0.94

The temperature models of transformations, hardness, volume fractions of ferrite, pearlite, bainite and martensite in a steel developed with the method of artificial neural networks were used in a computer software to calculate CCT diagrams. The program shown in the work [13] was modified. All functions performing calculations were replaced with a new source code based on neural networks herein. The input data to the program are mass concentrations of the elements and the austenititzing temperature that can be introduced by the user or calculated. The program calculates the austenitizing temperature based on Ac_3 temperature (by default: Ac_3+50°C). The austenitizing temperature also may be entered by the user. Figures 2-5 show the examples of CCT diagrams that are experimental

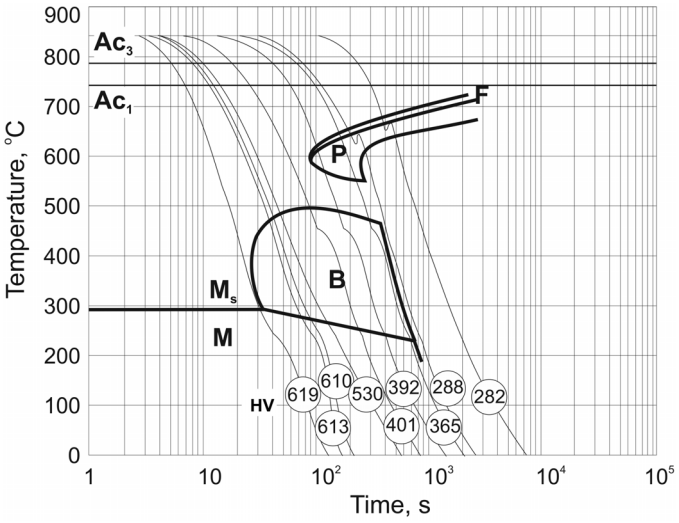

Fig. 2. CCT diagram determined experimentally for steel with a mass concentration of elements: 0.49%C, 0.9%Mn, 0.23%Si, 1.03%Cr, 0.21%V, austenitised at temperature of 840°C [14]

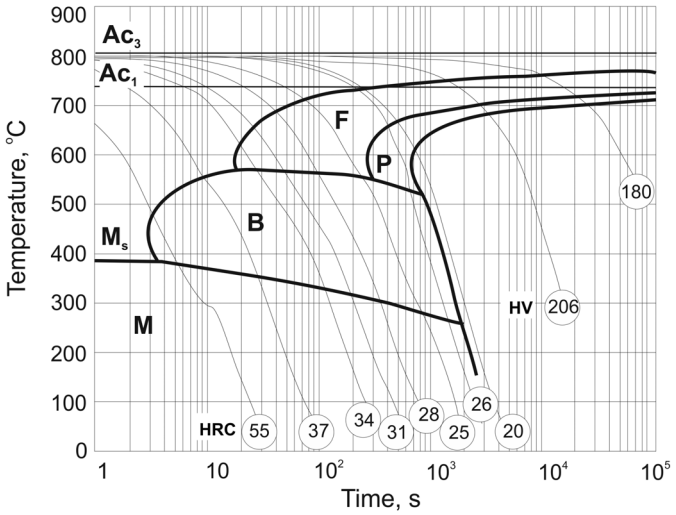

Fig. 3. CCT diagram determined experimentally for steel with a mass concentration of elements: 0.30%C, 0.64%Mn, 0.22%Si, 1.01%Cr, 0.11%Ni, 0.24%Mo, austenitised at temperature of 850°C [14]

and were calculated with a computer program. The diagrams presented in the article were chosen randomly from the verification data set. In order to compare the results of calculations with experimental diagrams, the austenitizing temperature such as in the experimental diagrams was used to calculate CCT diagrams.

In the Figures 4 and 5 it can be seen that the algorithm used to draw CCT diagrams requires some correction. The incorrect operation of the algorithm is visible for the start temperatures of transformation of austenite into ferrite (Fig. 4) as well as the finish temperatures of pearlitic transformation (Fig. 5). The problem may be solved by an increase in the number of cooling rates for which the temperature values of transformations are

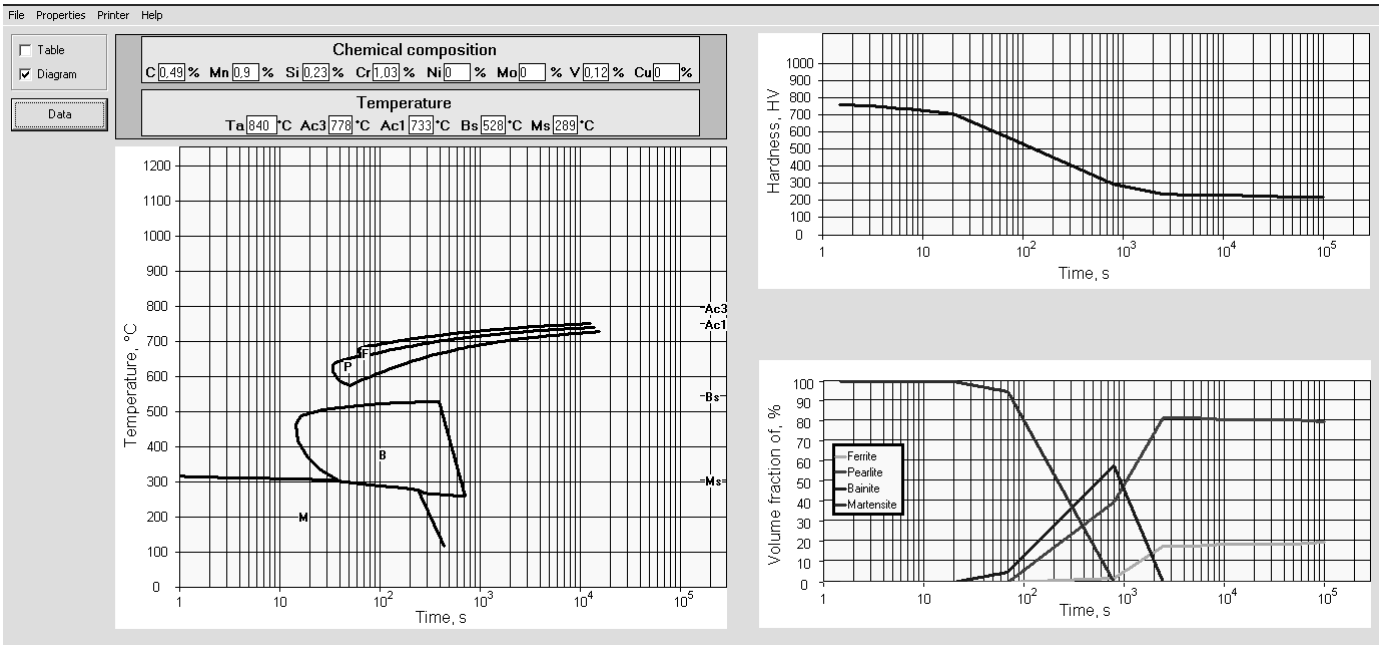

Fig. 4. CCT diagram calculated for steel with a mass concentration of elements: 0.49%C, 0.9%Mn, 0.23%Si, 1.03%Cr, 0.21%V, austenitised at temperature of 840°C

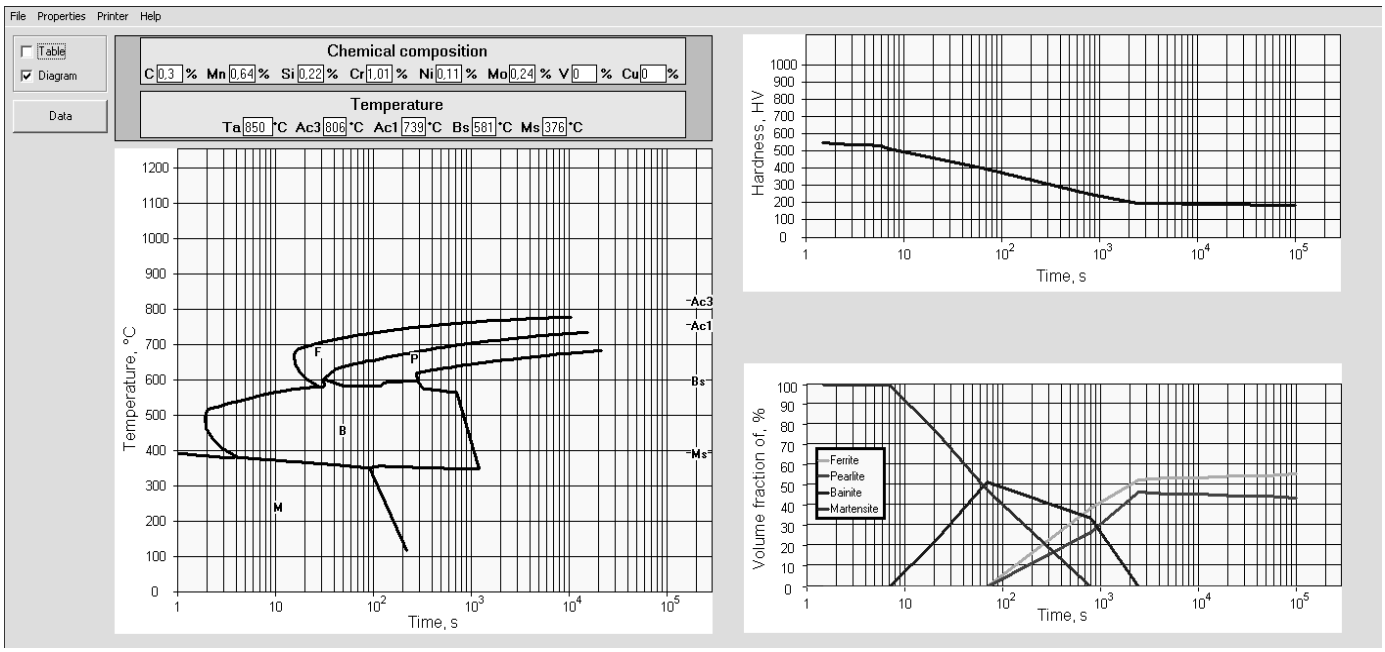

Fig. 5. CCT diagram calculated for steel with a mass concentration of elements: 0.30%C, 0.64%Mn, 0.22%Si, 1.01%Cr, 0.11%Ni, 0.24%Mo, austenitised at temperature of 850°C

calculated and the use of the results of these calculations to determine the trend line. Currently, work is underway to check this solution.

4. Summary

The paper shows the selected major information on the new neural model of CCT diagrams for structural and engineering steels. The detailed information on the set of experimental data, modelling method and statistics for review of the model, including the statistics for the verification set as well as information about the computer program are shown in the work [15].

The presented model of CCT diagrams forms 17 neural networks. In case of enlarging or modifying a set of CCT diagrams, training process of neural networks can be continued. Datasets for training and testing of neural networks and the computer program code was prepared so to allow their modification. The CCT diagram model was developed also with multiple regression and logistic regression. The modelling uses the same set of experimental data. Equations to calculate CCT diagrams are shown in the works [15-17]

The final modeling stage should be the experimental verification of developed dependencies so further work is planned connected with the experimental verification of calculations with a dilatometric method for commercial steels and model alloys.

The increasing popularity of computational intelligence methods in many fields of science and engineering is also reflected by the area of materials engineering [18-25].Use of hybrid methods is an important trend related to modelling in materials engineering [26-29]. The numerically verified models are used to calculate the chemical composition of steel with required transformation temperatures and hardness of steel cooled continuously from the austenitizing temperature. To identify mass concentrations of the elements, the hybrid method that uses artificial neural networks and the genetic algorithm were used. Method and results are shown in the work [15].

REFERENCES

[1] J.C. Zhao, M.R. Notis, Mater. Sci. Eng. **15**, 135-207 (1995).
[2] P. Payson, C.H. Savage, Steels Trans. ASM **33**, 261-275 (1944).
[3] A.B. Greninger, Steels Trans. ASM **30**, 1-26 (1942).
[4] A.B. Greninger, A.R. Troiano, Steel Trans. ASM **28**, 537-574 (1940).
[5] W. Vermeulen, P.F. Morris, A.P. De Weijer, S. Van der Zwaag, Ironmak. Steelmak. **23** (5), 433-437 (1996).
[6] W. Vermeulen, S. Van der Zwaag., P. Morris, T. De Weijer, Steel Res. **68** (2), 72-79 (1997).
[7] J. Wang, P.J. Van Der Wolk, S.J. Van Der Zwaag, J. Mater. Sci. **35** (17), 4393-4404 (2000), DOI: 10.1023/A:1004865209116.
[8] E.S. Davenport, E.S. Bain, T. Metall. Soc. AIME **90**, 117-154 (1930).
[9] J. Trzaska, PhD thesis, Methodology of the computer modelling of the supercooled austenite transformations of the constructional steels, Silesian University of Technology, Gliwice, Poland (2002), (in Polish).
[10] L.A. Dobrzański, J. Trzaska, Comp. Mater. Sci. **30** (3-4), 251-259 (2004), DOI: 10.1016/j.commatsci.2004.02.011.
[11] L.A. Dobrzański, J. Trzaska, Mater. Sci. Forum **437** (4), 359-362 (2003).
[12] J. Trzaska, Archives of Materials Science and Engineering **82 (**2), 62-69 (2016).

[13] J. Trzaska, L.A. Dobrzański, A. Jagiełło, Journal of Achievements in Materials and Manufacturing Engineering **24** (2), 171-174 (2007).

[14] G.F. Vander Voort (Ed.), Atlas of Time-Temperature Diagrams for Irons and Steels, ASM International (2004).

[15] J. Trzaska, Prediction methodology for the anisothermal phase transformation curves of the structural and engineering steels, Silesian University of Technology Press, Gliwice (2017), (in Polish).

[16] J. Trzaska, Arch. Metall. Mater. **60** (1), 181-185 (2015), DOI: 10.1515/amm-2015-0029.

[17] J. Trzaska, Journal of Achievements in Materials and Manufacturing Engineering **65** (1), 38-44 (2014).

[18] H.K.D.H. Bhadeshia, R.C. Dimitriu, S. Forsik, J.H. Pak, J.H. Ryu, Mater. Sci. Tech.-Lond. **25** (4), 504-510 (2009), DOI: 10.1179/174328408X311053.

[19] W. Sha, K.L. Edwards, Materials and Design **28**, 1747-1752 (2007), DOI: 10.1016/j.matdes.2007.02.009.

[20] L.A. Dobrzański, J. Trzaska, A.D. Dobrzańska-Danikiewicz, Use of Neural Networks and Artificial Intelligence Tools for Modeling, Characterization, and Forecasting in Material Engineering, in: S. Hashmi (Ed.), Comprehensive Materials Processing, Elsevier Science (2014), DOI: 10.1016/B978-0-08-096532-1.00215-6.

[21] P. Papliński, W. Sitek, J. Trzaska, Adv. Mat. Res. **1036**, 580-585 (2014), DOI: 10.4028/www.scientific.net/AMR.1036.580.

[22] L.A. Dobrzański, M. Drak, J. Trzaska, J. Mater. Process. Tech. **192-193**, 595-601 (2007), DOI: 10.1016/j.jmatprotec.2007.04.010.

[23] C. Capdevila, Neural networks modeling of phase transformations in steels, in: E. Pereloma, D.V. Edmonds (Eds.) Phase Transformations in Steels, Woodhead Publishing (2012), DOI: 10.1533/9780857096111.3.464.

[24] F. Nurnberger, M. Schaper, F.W. Bach, J. Mozgova, K. Kuznetsov, A. Halikova, O. Perederieieva, Adv. Mater. Sci. Eng. **1**, 1-10 (2009), DOI: 10.1155/2009/582739.

[25] W. Sitek, J. Trzaska, L.A. Dobrzański, Mater. Sci. Forum **575-578**, 892-897 (2008), DOI: 10.4028/www.scientific.net/MSF.575-578.892.

[26] N.S. Reddy, J. Krishnaiah, Hur Bo Young, Jae Sang Lee, Comp. Mater. Sci. **101**, 120-126 (2015), DOI: 10.1016/j.commatsci.2015.01.031.

[27] W. Sitek, Journal of Achievements in Materials and Manufacturing Engineering **39** (2), 115-160 (2010).

[28] W. Sitek, J. Trzaska, Journal of Achievements in Materials and Manufacturing Engineering **54** (1), 93-102 (2012).

[29] S. Chakraborty, P.P. Chattopadhyay, S.K. Ghosh, S. Datta, Appl. Soft. Comput. **58**, 297-306 (2017), DOI: 10.1016/j.asoc.2017.05.001.